

Complete power spectrum for an induced gravity open inflation model

Juan García-Bellido

*Astronomy Centre, University of Sussex, Falmer, Brighton BN1 9QH, United Kingdom
and Theory Division, CERN, CH-1211 Geneva 23, Switzerland*

Andrew R. Liddle

*Astronomy Centre, University of Sussex, Falmer, Brighton BN1 9QH, United Kingdom
(October 15, 2018)*

We study the phenomenological constraints on a recently proposed model of open inflation in the context of induced gravity. The main interest of this model is the relatively small number of parameters, which may be constrained by many different types of observation. We evaluate the complete spectrum of density perturbations, which contains continuum sub-curvature modes, a discrete super curvature mode, and a mode associated with fluctuations in the bubble wall. From these, we compute the angular power spectrum of temperature fluctuations in the microwave background, and derive bounds on the parameters of the model so that the predicted spectrum is compatible with the observed anisotropy of the microwave background and with large-scale structure observations. We analyze the matter era and the approach of the model to general relativity. The model passes all existing constraints.

PACS numbers: 98.80.Cq Preprint CERN-TH/96-302, SUSSEX-AST 96/10-2, astro-ph/9610183

I. INTRODUCTION

The inflationary paradigm [1] not only provides a solution to the classical problems of the hot big bang cosmology, but also predicts an almost scale invariant spectrum of metric perturbations which could be responsible for the observed anisotropy of the cosmic microwave background (CMB), as well as the origin of the large-scale structure. Present microwave background anisotropy experiments offer only weak constraints; for example the COBE satellite [2] gives a very accurate determination of the amplitude of large-angle anisotropies (which can be used to normalize theories) but only weakly constrains the shape of the spectrum. Information is beginning to come in on degree scales, and from combining microwave anisotropy constraints with those from large-scale structure, but the present situation still offers considerable freedom. However, we can expect this to change dramatically in the near future, especially with the launch of new-generation microwave anisotropy satellites *MAP* [3] and *COBRAS/SAMBA* [4] which promise to measure both cosmological parameters such as Ω_0 , H_0 and Ω_B , and parameters associated with the primordial spectra to great accuracy [5]. It is therefore desirable to provide a variety of inflationary models with definite predictions, which could be used to test and exclude them.

Until recently, inflation was always associated with a flat universe, due to its ability to drive the spatial curvature so effectively to zero. However, it is now understood that inflation comprises a wider class of models, some of which may give rise to an open universe at present [6–8]. Observations suggesting a high value of the Hubble parameter, such as those using the Hubble Space Telescope [9], have motivated the idea of consider-

ing a low-density universe, in an attempt to make the age compatible with globular cluster ages. Most frequently a cosmological constant is introduced to restore spatial flatness, but open inflation models (see Ref. [10] for an introduction) offer the alternative of a genuinely open universe. Such models generically contain a field trapped in a false vacuum which tunnels to its true vacuum via nucleation of a single bubble, inside which a second period of inflation drives the universe to almost flatness. This way one solves the homogeneity problem independently from the flatness problem, allowing for an open homogeneous universe inside the bubble.

In an open universe, the analysis of density perturbations and microwave anisotropies is considerably more complicated than in the usual flat space case. Early studies by Lyth and Stewart [11] and by Ratra and Peebles [12] evaluated the spectrum for slow-roll models leading to an open Universe, using the conformal vacuum as an initial condition. In the single-bubble models a different vacuum choice is appropriate, leading to a slightly different spectrum [13,7]. It was later realised however that extra perturbations, with discrete wavenumbers, can also be generated. In all, three different types of perturbation have been identified: a continuous spectrum of modes with wavenumber k greater than the curvature scale, known as sub-curvature modes; a super-curvature mode associated with the open de Sitter vacuum [13,14], and a mode associated with perturbations in the bubble wall at tunneling [15–17]. The observed large-scale structures are due to the sub-curvature modes, but large-angle microwave anisotropies are generated by all three types, with observations seeing the combined total anisotropy. The first computation of all three types of mode together for a particular model was made in Ref. [15] for arbitrary

Ω_0 in the context of the two-field models of Linde and Mezhlumian [8]. Later on, a thorough calculation of all three contributions from the point of view of quantum field theory in open de Sitter space was carried out by Yamamoto et al. [17] (see also Ref. [18]). Here we shall carry out a similar calculation for a different two-field model, for which we shall also discuss some of the implications of large-scale structure observations.

In addition to scalar metric perturbations, we expect open inflation to lead to the production of a gravitational wave spectrum, as in conventional inflationary models. Unfortunately, no-one has yet formulated a method of calculating this spectrum even approximately, and so we shall not be able to consider them here. In chaotic inflation models, gravitational waves are negligible in the slow-roll limit (see e.g. Ref. [19]); one can hope that this is also true in the open inflation case, but that remains to be confirmed.

The particular open inflation model we shall study, introduced in Ref. [20], is based on the induced gravity Lagrangian [21]. The interest of this model is the relatively small number of parameters, which can be constrained by several different types of observation. The inflaton is a dilaton field, whose vacuum expectation value at the end of inflation determines the present value of the gravitational constant. We will constrain the model from CMB and large-scale structure observations, as well as ensuring that post-Newtonian and oscillating gravitational coupling bounds are satisfied.

II. THE MODEL

We consider the model of Ref. [20], with an induced gravity Lagrangian [21]

$$\mathcal{L} = \frac{1}{2}\xi\varphi^2 R - \frac{1}{2}\partial_\mu\varphi\partial^\mu\varphi + V(\varphi) + \mathcal{L}_{\text{mat}}. \quad (1)$$

The dilaton field φ determines the effective gravitational coupling, which is positive for $\xi > 0$. In the absence of a potential, this action corresponds to the usual Brans–Dicke action [22], where

$$\Phi = 8\pi\xi\varphi^2, \quad \omega = \frac{1}{4\xi}. \quad (2)$$

The Einstein and scalar field equations are [23,24]

$$-\xi\varphi^2 G_{\mu\nu} = g_{\mu\nu}V(\varphi) + \xi(\nabla_\mu\nabla_\nu - g_{\mu\nu}\nabla^2)\varphi^2 + \left(\partial_\mu\varphi\partial_\nu\varphi - \frac{1}{2}g_{\mu\nu}(\partial\varphi)^2\right) + T_{\mu\nu}, \quad (3)$$

and

$$\nabla^2\varphi = -V'(\varphi) + \xi\varphi R, \quad (4)$$

where $G_{\mu\nu}$ is the Einstein tensor. Using the identities $G_{\mu\nu}{}^{;\nu} = 0$ and $R_{\mu\nu}\nabla^\nu\Phi = \nabla_\mu(\nabla^2\Phi) - \nabla^2(\nabla_\mu\Phi)$, together with the φ equation of motion, we find that the energy-momentum tensor is conserved,

$$T_{\mu\nu}{}^{;\nu} = 0, \quad (5)$$

even in the presence of a potential for the scalar field. Substituting R into the equation of motion of the scalar field, we obtain

$$\frac{1}{2}(1 + 6\xi)\nabla^2\varphi^2 = 4V(\varphi) - \varphi V'(\varphi) + T^\lambda{}_\lambda. \quad (6)$$

We will consider a potential of the type [21,20]

$$V(\varphi) = \frac{\lambda}{8}(\varphi^2 - \nu^2)^2. \quad (7)$$

During a radiation dominated era $T^\lambda{}_\lambda = 0$ and the scalar field will sit at its minimum; matching the present-day Planck mass demands

$$8\pi\xi\nu^2 = m_{\text{Pl}}^2. \quad (8)$$

During a matter era, the scalar field oscillates around its minimum with a large frequency and negligible amplitude, passing all the tests associated with an oscillating gravitational coupling [25] as we will show in Section VII.

III. INDUCED GRAVITY OPEN INFLATION

In the induced gravity open inflation model [20], the initial period of inflation is driven by the false vacuum energy of a second scalar field σ . This energy density is able to hold the dilaton at a fixed location displaced from the minimum of its potential. After the false vacuum decays, the rolling of the dilaton to its minimum drives the second period of inflation necessary to give Ω_0 in the desired range.

A. False vacuum inflation

Initially the scalar field σ is in its false vacuum. The details of its potential are not particularly important; we will parametrize them later. In the false vacuum, the universe expands driving the spatial curvature and any previous inhomogeneities to zero. Later on, the σ field tunnels to its true minimum at $V(\sigma) = 0$, via the production of a bubble.

The equations of motion of the dilaton field before and after the tunneling can be written as [20]

$$H^2 + 2H\frac{\dot{\varphi}}{\varphi} + \frac{K}{a^2} = \frac{1}{3\xi\varphi^2} \left[\frac{1}{2}\dot{\varphi}^2 + V(\varphi) + V(\sigma) \right], \quad (9)$$

$$\ddot{\varphi} + 3H\dot{\varphi} + \frac{\dot{\varphi}^2}{\varphi} = \frac{4V(\varphi) - \varphi V'(\varphi) + 4V(\sigma)}{(1 + 6\xi)\varphi}. \quad (10)$$

Here $V(\sigma) = V_0$ in the false vacuum and vanishes in the true vacuum, while the curvature K is effectively zero before tunnelling and is negative afterwards. The basis

for the open inflation model is the existence of a stable static solution in the false vacuum [20], with

$$\varphi_{\text{st}}^2 = \nu^2 \left(1 + \frac{8V_0}{\lambda\nu^4}\right) \equiv \nu^2 (1 + \alpha), \quad (11)$$

$$H_{\text{st}}^2 = \frac{8\pi V_0}{3m_{\text{Pl}}^2}. \quad (12)$$

Its stability is best seen in the Einstein frame [20]. Under the transformation

$$dt = \frac{\nu}{\varphi} d\tilde{t}, \quad a(t) = \frac{\nu}{\varphi} \tilde{a}(\tilde{t}), \quad (13)$$

$$\frac{\dot{\phi}}{\nu} = (1 + 6\xi)^{1/2} \ln \frac{\varphi}{\nu}, \quad (14)$$

the effective potential in the false vacuum becomes

$$U_{\text{F}}(\phi) = \frac{\lambda\nu^4}{8} \left[1 - 2\frac{\nu^2}{\varphi^2} + (1 + \alpha)\frac{\nu^4}{\varphi^4}\right], \quad (15)$$

$$U'_{\text{F}}(\phi) = \frac{\lambda\nu^3}{2(1 + 6\xi)^{1/2}} \frac{\nu^2}{\varphi^2} \left[1 - (1 + \alpha)\frac{\nu^2}{\varphi^2}\right], \quad (16)$$

$$U''_{\text{F}}(\phi) = \frac{\lambda\nu^2}{1 + 6\xi} \frac{\nu^2}{\varphi^2} \left[2(1 + \alpha)\frac{\nu^2}{\varphi^2} - 1\right], \quad (17)$$

where primes denote derivatives with respect to the Einstein-frame scalar field ϕ . It is clear that $U'_{\text{F}}(\phi_{\text{st}}) = 0$ at the static value, while the effective square mass is positive ensuring stability. At the static point, we have

$$H_{\text{F}}^2 = \frac{8\pi U_{\text{F}}}{3m_{\text{Pl}}^2} = \frac{\lambda\nu^2}{24\xi} \frac{\alpha}{1 + \alpha}, \quad (18)$$

$$m_{\text{F}}^2 \equiv U''_{\text{F}}(\varphi_{\text{st}}) = \frac{\lambda\nu^2}{1 + 6\xi} \frac{1}{1 + \alpha}, \quad (19)$$

where H_{F} is the rate of expansion of the universe in the Einstein frame and m_{F} is the mass of the ϕ field at the static point.

B. True vacuum inflation

Eventually the σ field tunnels to its true vacuum by nucleating a bubble, inside which the universe inflates to almost flatness. A sufficiently low tunneling rate ensures that the bubble stays isolated [26,20]. After tunneling, the effective potential in the true vacuum, again in the Einstein frame, becomes

$$U_{\text{T}}(\phi) = \frac{\lambda\nu^4}{8} \left(1 - \frac{\nu^2}{\varphi^2}\right)^2, \quad (20)$$

$$U'_{\text{T}}(\phi) = \frac{\lambda\nu^3}{2(1 + 6\xi)^{1/2}} \frac{\nu^2}{\varphi^2} \left(1 - \frac{\nu^2}{\varphi^2}\right), \quad (21)$$

$$U''_{\text{T}}(\phi) = \frac{\lambda\nu^2}{1 + 6\xi} \frac{\nu^2}{\varphi^2} \left(2\frac{\nu^2}{\varphi^2} - 1\right). \quad (22)$$

The minimum of the potential is now at $\varphi = \nu < \varphi_{\text{st}}$, and the field slow-rolls from φ_{st} driving a second stage of inflation. The dynamics of this situation were investigated long ago in Ref. [27]. The rate of expansion and effective mass in the true vacuum immediately after tunneling are

$$H_{\text{T}}^2 = \frac{8\pi U_{\text{T}}}{3m_{\text{Pl}}^2} - \frac{K}{a^2} = \frac{\lambda\nu^2}{24\xi} \left(\frac{\alpha}{1 + \alpha}\right)^2 - \frac{K}{a^2}, \quad (23)$$

$$m_{\text{T}}^2 \equiv U''_{\text{T}}(\varphi_{\text{st}}) = \frac{\lambda\nu^2}{1 + 6\xi} \frac{1 - \alpha}{(1 + \alpha)^2}. \quad (24)$$

The curvature term quickly becomes negligible as the second phase of inflation progresses.

For later use, we also define the usual slow-roll parameters [19] soon after tunneling

$$\epsilon \equiv \frac{m_{\text{Pl}}^2}{16\pi} \left(\frac{U'_{\text{T}}(\phi)}{U_{\text{T}}(\phi)}\right)^2 = \frac{8\xi}{1 + 6\xi} \frac{1}{\alpha^2}, \quad (25)$$

$$\eta \equiv \frac{m_{\text{Pl}}^2}{8\pi} \frac{U''_{\text{T}}(\phi)}{U_{\text{T}}(\phi)} = \frac{8\xi}{1 + 6\xi} \frac{1 - \alpha}{\alpha^2}. \quad (26)$$

The scalar field ϕ slow-rolls down the effective potential given by Eq. (20) until it starts oscillating around its minimum and inflation ends. The value of ϕ at the end of inflation can be computed from the condition $-\dot{H}_{\text{T}} \simeq H_{\text{T}}^2$ (or equivalently $\dot{\phi}^2 \simeq U_{\text{T}}(\phi)$), giving

$$\varphi_{\text{end}}^2 = \nu^2 \left(1 + \frac{8\xi}{1 + 6\xi}\right) \equiv \nu^2 (1 + \beta). \quad (27)$$

The number of e -folds during the second stage of inflation from ϕ_{st} to ϕ_{end} can be computed in the Einstein frame,

$$N = \frac{1}{\xi\nu^2} \int_{\phi_{\text{end}}}^{\phi_{\text{st}}} \frac{d\phi U_{\text{T}}(\phi)}{U'_{\text{T}}(\phi)} = \frac{1}{\beta} \left[\alpha - \beta - \ln\left(\frac{1 + \alpha}{1 + \beta}\right)\right]. \quad (28)$$

In order to produce an open universe, the number of e -folds after tunneling has to be around $N = 60$, the precise number depending on the reheating temperature and other details of the post-inflationary evolution. We adopt the number 60 for definiteness. This gives a relation between the two dimensionless parameters α and β .

IV. METRIC PERTURBATIONS AND TEMPERATURE ANISOTROPIES

Quantum fluctuations of the inflaton field ϕ produce long-wavelength curvature perturbations; we will use \mathcal{R} to denote the curvature perturbation on comoving hypersurfaces (in the Einstein frame).

Open inflation generates three different types of modes: those that cross outside during the second stage of inflation and constitute a continuum of sub-curvature modes;

a discrete super-curvature mode associated with the open de Sitter vacuum, and a mode associated with the bubble wall fluctuations at tunneling. The mode functions are eigenvalues of the Laplacian, with eigenvalue $-k^2$ where k is the wavenumber. Defining $q^2 = k^2 - 1$, then the sub-curvature modes have positive q^2 and the other modes have negative q^2 . We label the former mode functions $\Pi_{ql}(r)$ and the latter $\bar{\Pi}_{|q|l}(r)$. In Appendix A we give explicit forms for these; see also Ref. [28].

The spectrum $\mathcal{P}_{\mathcal{R}}(q)$ of the curvature perturbation can be defined from the mode expansion of \mathcal{R} by [14]

$$\langle \mathcal{R}_{qlm} \mathcal{R}_{q'l'm'} \rangle = \frac{2\pi^2}{q(q^2 + 1)} \mathcal{P}_{\mathcal{R}}(q) \delta(q - q') \delta_{ll'} \delta_{mm'}. \quad (29)$$

In order to compare with observations, we must compute the effect that such a perturbation has on the temperature of the CMB, expanded as usual in spherical harmonics

$$\frac{\Delta T}{T}(\theta, \phi) = \sum_{lm} a_{lm} Y_m^l(\theta, \phi). \quad (30)$$

The main contribution on large scales comes from the Sachs–Wolfe effect [29]. The complete angular power spectrum $C_l \equiv \langle |a_{lm}|^2 \rangle$ has contributions from the continuum of sub-curvature modes, the super-curvature mode and the bubble-wall mode,

$$C_l = C_l^{(C)} + C_l^{(S)} + C_l^{(W)}. \quad (31)$$

The contribution of each mode to the C_l is measured by a window function W_{ql} , given by [29]

$$5 W_{ql} = \Pi_{ql}(\eta_0) + 6 \int_0^{\eta_0} dr F'(r) \Pi_{ql}(r), \quad (32)$$

for the sub-curvature modes; the same expression with $\bar{\Pi}_{|q|l}$ gives the window function $\bar{W}_{|q|l}$ for the negative q^2 modes. Here

$$F(\eta) = 5 \frac{\sinh^2 \eta - 3\eta \sinh \eta + 4(\cosh \eta - 1)}{(\cosh \eta - 1)^3}, \quad (33)$$

gives the growth rate of perturbations during the matter era [30], and $\eta_0 = \cosh^{-1}(2/\Omega_0 - 1)$ is the distance to the last scattering surface. The normalization of the contribution to the C_l is given in the expressions below.

Sub-curvature modes

A detailed computation of the amplitude of the sub-curvature modes gives the result [13,7,17]

$$\mathcal{P}_{\mathcal{R}}(q) = \coth(\pi q) \frac{8 U_{\text{T}}}{3 \epsilon m_{\text{Pl}}^4}, \quad (34)$$

where ϵ is the slow-roll parameter defined earlier and we have dropped a small correction term from the change in

mass during tunneling [17]. The $\coth(\pi q)$ factor can be interpreted as due to the initial transient behavior as the curvature term dies away.

Notice that Eq. (34) has only been derived in the case of perfect de Sitter expansion after tunneling [17]. It seems very plausible that it also holds when there are deviations from de Sitter, where the right hand side is to be evaluated when $k = aH$. This is the only simple formula which reduces to the correct result both for de Sitter expansion and in the flat-space limit (see e.g. Ref. [31]) which must be attained after the curvature term has died away sufficiently.

Following normal practice, we describe the variation in the spectrum caused by the time variation of H and ϵ by a power-law. Notice that this power-law is superimposed on the \coth behavior, so the complete spectrum does not have a power-law form on very large scales. The power-law index of $\mathcal{P}_{\mathcal{R}}(q)/\coth(\pi q)$ can be derived in the usual way from the slow-roll parameters as [19]

$$n - 1 = -6\epsilon + 2\eta = -\frac{8\xi}{1 + 6\xi} \frac{2(2 + \alpha)}{\alpha^2}, \quad (35)$$

and gives the standard result in the flat-space limit where the \coth term in Eq. (34) equals unity. This expression is valid provided both ϵ and $|\eta|$ are much less than one.

For later comparison, we write the spectrum as

$$\mathcal{P}_{\mathcal{R}}(q) = A_{\text{C}}^2 \coth(\pi q) [1 + q^2]^{(n-1)/2}, \quad (36)$$

where

$$A_{\text{C}}^2 = \frac{8 U_{\text{T}}(\phi_{\text{st}})}{3 \epsilon(\phi_{\text{st}}) m_{\text{Pl}}^4} \quad (37)$$

is a measure of the amplitude at the $q = 0$ limit. Formally the spectrum diverges there, though not in a harmful way thanks to the window function given by Eq. (32).

For our model, Eq. (37) becomes

$$A_{\text{C}}^2 = \frac{\lambda}{(16\pi\xi)^2} \frac{1 + 6\xi}{6\xi} \left(\frac{\alpha^2}{1 + \alpha} \right)^2. \quad (38)$$

The angular power spectrum for the continuum modes can be written as [13]

$$C_l^{(C)} = 2\pi^2 \int_0^\infty \frac{dq}{q(1 + q^2)} \mathcal{P}_{\mathcal{R}}(q) W_{ql}^2. \quad (39)$$

We compute the angular power spectrum for different values of Ω_0 in the low-density range $0.2 \leq \Omega_0 \leq 0.6$. In Fig. 1 we show the first twelve multipoles, adopting the notation $D_l = l(l + 1) C_l$.*

*Our calculation only includes the Sachs–Wolfe effect, as is appropriate for computing the amplitude on the largest angular scales. We therefore don't include the rise to the acoustic peak, caused by the first oscillation of the photon–baryon fluid, which is known to induce an effective extra tilt of around 0.15 [32]; see for example Fig. 8 in Ref. [33] (who only consider sub-curvature modes).

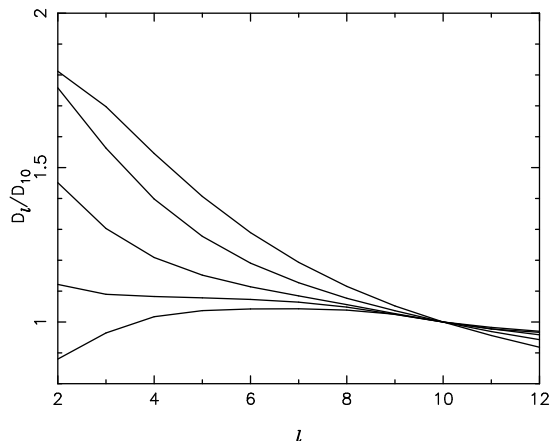


FIG. 1. The first 12 multipoles of the angular power spectrum associated with the continuum modes, normalized to the tenth multipole, for $\Omega_0 = 0.2, 0.3, 0.4, 0.5, 0.6$ as read from top to bottom at low l .

The normalization to COBE for tilted open models has recently been given by Bunn and White [33], under the assumption that only the continuum modes are important. They specify a quantity δ_H , which measures the normalization of the present matter power spectrum. The preferred value depends on n and Ω_0 ; however our model is nearly scale-invariant and the dependence on Ω_0 is quite weak and can be ignored at the accuracy we are working. Therefore we take the value $\delta_H = 2 \times 10^{-5}$ regardless of Ω_0 . In an open universe δ_H is related to $\mathcal{P}_{\mathcal{R}}$ as [33]

$$\delta_H = \frac{2}{5} \mathcal{P}_{\mathcal{R}}^{1/2} \frac{g(\Omega_0)}{\Omega_0}, \quad (40)$$

where $g(\Omega_0)$ is a function measuring the suppression in the growth perturbations relative to a critical-density universe, and $\mathcal{P}_{\mathcal{R}}$ is evaluated at around the 10th multipole where $\coth(\pi q) \simeq 1$. The Ω_0 dependence can give a factor of up to 1.5 in the region of interest, but we can ignore it as we do not require such accuracy. Reproducing the amplitude of temperature anisotropies is the main constraint on the parameters of the model, and yields

$$\sqrt{\lambda} = 6 \times 10^{-3} \left(\frac{\xi^3}{1 + 6\xi} \right)^{1/2} \frac{1 + \alpha}{\alpha^2}, \quad (41)$$

as found in Ref. [20]. This relation can readily be satisfied for reasonable values of the parameters [20].

Super-curvature mode

We now consider the contribution to the CMB anisotropies coming from the discrete super-curvature mode associated with the dilaton field ϕ . This mode appears in the open de Sitter spectrum when $m_{\mathbb{F}}^2 < 2H_{\mathbb{F}}^2$ in the false vacuum [13]. The tunneling field σ does not have this

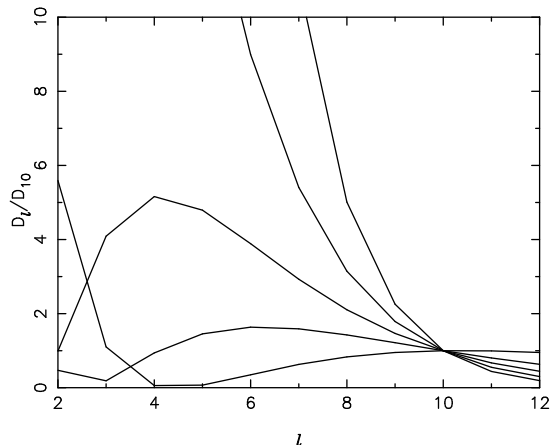


FIG. 2. As Fig. 1, but for the discrete supercurvature mode, showing $\Omega_0 = 0.6, 0.5, 0.4, 0.3, 0.2$, reading from top to bottom at in the centre of the figure.

mode in its spectrum, since its mass at the false vacuum should be much larger than the rate of expansion in order to prevent tunneling via the Hawking-Moss instanton [8]. The wavenumber associated with this mode is given by

$$k^2 = 1 - \left[\left(\frac{9}{4} - \frac{m_{\mathbb{F}}^2}{H_{\mathbb{F}}^2} \right)^{1/2} - \frac{1}{2} \right]^2. \quad (42)$$

The amplitude of this mode is [18]

$$A_S^2 \simeq \frac{8 U_{\mathbb{F}}}{3 \epsilon m_{\mathbb{P}}^4} = A_C^2 \frac{U_{\mathbb{F}}}{U_{\mathbb{T}}}. \quad (43)$$

where the normalization of A_S^2 is defined through the formula for the angular power spectrum of temperature anisotropies induced by this super-curvature mode, namely [17,18]

$$D_l^{(S)} \equiv l(l+1) C_l^{(S)} = 4\pi A_S^2 \bar{W}_{1l}^2. \quad (44)$$

Fig. 2 shows the first twelve multipoles, showing quite a complicated dependence. For example, it is not automatic that the quadrupole receives the biggest contribution [34].

More important than the shape is the amplitude of these anisotropies relative to the sub-curvature ones. We will compare their contributions in Section V.

Bubble wall mode

In addition to the sub- and super-curvature modes, there is a contribution from the bubble wall fluctuations. These fluctuations contribute as a transverse traceless curvature perturbation mode with $k^2 = -3$, see Refs. [15–17], which still behaves as a homogeneous random field [35,28].

Unlike the modes we've discussed so far, these modes need extra parameters for their description, because their

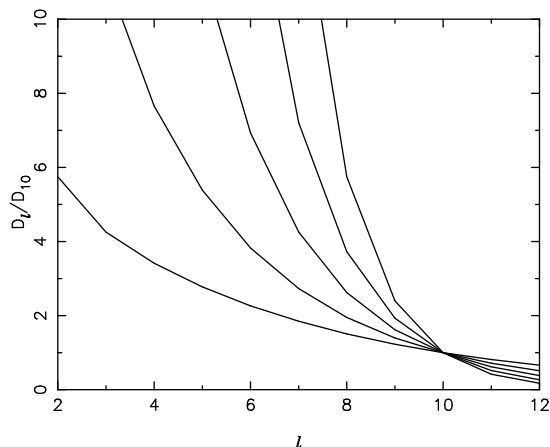


FIG. 3. As Fig. 1, but for the discrete bubble wall mode, for $\Omega_0 = 0.6, 0.5, 0.4, 0.3, 0.2$, from top to bottom at low l .

amplitude depends on the details of the bubble wall, which is determined by the potential for the σ field. This extra freedom allows the bubble wall fluctuations to be tuned relative to the others.

The perturbation amplitude for the bubble wall mode is given by [15,36,17]

$$A_W^2 = \frac{4U_T}{a^2 b m_{\text{Pl}}^4} \left[a^2 + (1 + a^2 b)^2 \right]^{1/2}, \quad (45)$$

where

$$a^2 = \frac{24\pi U_T S_1^2}{m_{\text{Pl}}^2 (U_F - U_T)^2}, \quad b = \frac{U_F - U_T}{4U_T}. \quad (46)$$

and S_1 gives the bubble wall contribution to the bounce action, $B_{\text{wall}} = 2\pi^2 R^3 S_1$ (see e.g. Ref. [15]). In order to compute S_1 , we will consider a symmetry breaking potential of the type

$$U(\sigma) = U_F + \frac{\gamma}{4} \sigma^2 (\sigma - \sigma_0)^2 - \mu U_0 \left(\frac{\sigma}{\sigma_0} \right)^4, \quad (47)$$

where $\sigma_0 = M\sqrt{2/\gamma}$ corresponds to the true vacuum and $U_0 = M^4/16\gamma$ is the value of potential at the maximum. With $\mu \ll 1$ for the thin-wall approximation to be valid, S_1 can be computed as [15]

$$S_1 = \int_0^{\sigma_0} d\sigma [2(U(\sigma) - U_F)]^{1/2} \simeq \frac{M^3}{3\gamma}. \quad (48)$$

In the limit $a^2 b \ll 1$ of small gravitational effects at tunneling, we recover the result of Ref. [8], namely

$$A_W^2 = \frac{2U_T(U_F - U_T)}{\pi m_{\text{Pl}}^2 S_1^2} = A_C^2 \frac{3\epsilon}{2a^2 b}, \quad (49)$$

where ϵ is the slow-roll parameter. However, in the opposite limit of strong gravitational effects, $a^2 b \gg 1$, we have [15]

$$A_W^2 = \frac{4U_T}{m_{\text{Pl}}^4} = A_C^2 \frac{3\epsilon}{2}, \quad (50)$$

which is much smaller than the amplitude of the continuum modes.

The angular power spectrum associated with the bubble wall mode is [15]

$$D_l^{(W)} \equiv l(l+1) C_l^{(W)} = \frac{4\pi A_W^2}{(l+2)(l-1)} \bar{W}_{2l}^2. \quad (51)$$

Fig. 3 shows the first twelve multipoles. The quadrupole has the largest amplitude for all Ω_0 .

We will compare their contribution to the CMB in the next Section.

V. COMPARISON WITH OBSERVATIONS

A. Microwave background anisotropies

We can now examine constraints on the shape of the combined spectrum. The COBE data alone do not offer particularly strong constraints in this respect; for example, although Yamamoto and Bunn [37] argued that the inclusion of super-curvature modes could harm the fit to COBE based on the two-year data, a recent comprehensive analysis of the four-year data by Górski et al. [38] finds no useful constraint. Those papers however discussed only a particular model for the super-curvature modes and didn't include the bubble-wall modes at all. As Sasaki and Tanaka discussed [18], there can be interesting constraints if the super-curvature modes have their amplitude enhanced, and we shall also see that the bubble wall modes are typically more important than the super-curvature ones.

Unfortunately, the complicated structure of the perturbation spectra in open inflation models means that for a full analysis each model would have to be confronted with the COBE data set on a case-by-case basis. Such an analysis is outside the scope of this paper. We shall adopt a more simplistic approach, which is to demand that the discrete modes do not dominate the quadrupole while contributing negligibly to the tenth multipole. This would give an unacceptable shape to the spectrum on the scales sampled by COBE.

In Fig. 4, we show the contributions to the quadrupole and to the tenth multipole, as functions of Ω_0 , normalized to the size of the corresponding metric perturbation. It does not require much effort to keep the contribution to the tenth multipole from the discrete modes low (unless Ω_0 is very small), but we must ensure that the quadrupole is not dominated by the discrete modes.

Considering first the super-curvature modes, across the whole range of interesting Ω_0 we find that the super-curvature mode contributes about a factor thirty less to the low multipoles than do the continuum modes,

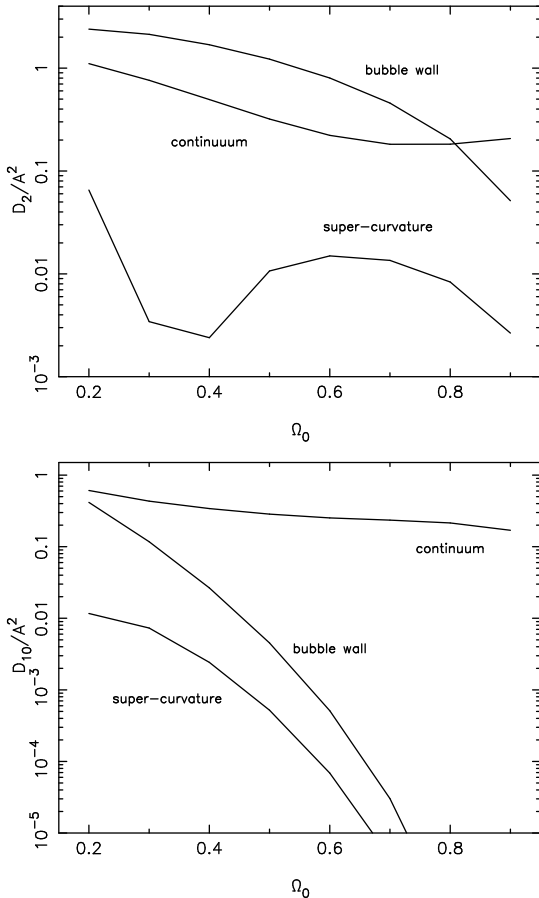


FIG. 4. The multipoles associated with each of the modes, normalized to the corresponding metric perturbation (A_C^2 , A_S^2 or A_W^2 as appropriate), as a function of Ω_0 . The top panel shows the quadrupole, while the lower shows the tenth multipole.

for the same size of metric perturbation.[†] Unless Ω_0 is very small, then if the super-curvature mode contribution is comparable to that of the continuum modes for the quadrupole, then it is negligible at the tenth multipole. Conservatively then, we shall require

$$A_S^2 \lesssim 100 A_C^2, \quad (52)$$

independently of Ω_0 , to prevent the super-curvature modes from dominating the low multipoles. In principle this limit could become inappropriate at small enough Ω_0 , because then the shape of the super-curvature spectrum is not so steep as to be ruled out by observations. However, by then the super-curvature modes are con-

[†]Although there is a dip around $\Omega_0 \simeq 0.4$ caused by an ‘accidental’ cancellation between intrinsic and line-of sight terms, the dip is not at the same location for the $l = 3, 4, \dots$ multipoles so the dip doesn’t allow one to weaken the constraint in its neighborhood [34].

tributing substantially even to the tenth multipole, and this will force down the normalization of COBE and make it impossible to fit large-scale structure observations. We can therefore adopt the above constraint even at low Ω_0 values. This imposes only a very mild constraint on the parameters of the model, namely

$$\alpha > 0.01, \quad (53)$$

which is easy to satisfy as we will see in Section VI. Since the value of Ω_0 at present is not known with any reasonable accuracy, it would be excessive to give a precise Ω_0 -dependent constraint. However, in the future, with a narrow range of values for Ω_0 , one would be able to give a more refined constraint on the parameters of the model from a full comparison of the detailed spectrum against COBE or its successors.

The same arguments can be applied to the bubble-wall modes; again we must prevent the domination of the quadrupole by these modes. For the interesting Ω_0 values (i.e. those not too close to one), we see from Fig. 4 that this simply requires

$$A_W^2 \lesssim A_C^2, \quad (54)$$

again independent of Ω_0 in the interesting range. This again imposes only a very mild constraint on the parameters of the model. For $a^2 b \ll 1$, we have $3\epsilon < 2a^2 b$ giving

$$\gamma < 9 \times 10^4 \frac{1 + 6\xi}{6\xi} \frac{M^3}{m_{\text{Pl}}^3} \alpha^{5/2}, \quad (55)$$

which is easy to satisfy for sufficiently large M . For $a^2 b \gg 1$, the amplitude of the metric perturbation Eq. (50) is completely negligible since $\epsilon \ll 1$, see Section VI.

B. Implications for large-scale structure

We can now combine the COBE normalization with observations of large-scale structure. This has the advantage of being relatively insensitive to the inclusion of super-curvature or bubble-wall modes, because with the constraints above these modes affect only the lowest multipoles, and while these can influence whether or not the spectral shape is a good fit to observations, they are not very significant at the higher multipoles (around the tenth to fifteenth) which are most important for determining the normalization. The drawback though is that looking to large-scale structure introduces a dependence on all the other cosmological parameters, namely the Hubble parameter h , the baryon density Ω_B and the nature of the dark matter. Despite this, interesting constraints can still be found, and two analyses have appeared which discuss tilted open models — Liddle et al. [39] who used the two-year COBE data and, more

recently, White and Silk [40] who used an accurate normalization to the four-year COBE data. Both of these considered only cold dark matter; other choices tend to strengthen the constraints so we shall do likewise.

In the model we are considering, the spectral index is always tilted to n less than one, as seen from Eq. (35). Whether or not this is allowed depends quite sensitively on both Ω_0 and h . If Ω_0 is too low, below around 0.30, then the open cold dark matter model fares badly against observations; this conclusion is consistent with a similar constraint from velocity flows [41] which is independent of the power spectrum. For example, White and Silk [40] find that this value is allowed only if the power spectrum is ‘blue’, with n at least 1.10. This conclusion is enforced both by the cluster abundance and by the shape of the galaxy correlation function. Our model will therefore be ruled out if it turns out that the universe is indeed as open as this.

However, one does not have to increase Ω_0 by very much to radically change this conclusion. For $\Omega_0 = 0.5$, for example, White and Silk find viable models for n as low as 0.85, with the preferred value depending on the Hubble parameter h . Our model can therefore be comfortably compatible with the data for this Ω_0 , and at least marginally compatible for Ω_0 as low as 0.4.

VI. TWO POSSIBLE SCENARIOS

In this section we will explore two different scenarios.

A. $\xi \ll 1$

This case was considered in Ref. [20]. Here the dilaton expectation value ν is much larger than the present Planck mass, see Eq. (8). For definiteness, we will choose a particular value, $8\xi = 1/200$. From the required number of e -folds, Eq. (28), this determines α to be of order one.

Let us study now the contribution of the different modes to the CMB anisotropies. We first consider the continuum spectrum of sub-curvature modes. The slow-roll parameters, given by Eqs. (25) and (26), become

$$\epsilon \simeq \frac{1}{200}, \quad \eta \simeq 0, \quad (56)$$

which determine the tilt of the primordial spectrum of density perturbations via Eq. (35) as

$$n - 1 \simeq -6\epsilon \simeq -0.03, \quad (57)$$

which is compatible with large- and small-scale observations for $\Omega_0 \gtrsim 0.4$, according to Ref. [40]. The constraint on the amplitude of the angular power spectrum determines the value of λ via Eq. (41) as

$$\lambda \simeq 2.5 \times 10^{-5} \frac{6\xi^3}{1 + 6\xi} \simeq 4 \times 10^{-14}. \quad (58)$$

See Ref. [20] for a range of values, under the assumption $\xi \ll 1$.

We now consider the de Sitter vacuum super-curvature mode. This mode exists, since $m_{\text{P}}^2 < 2H_{\text{P}}^2$ for $\xi \ll 1$ from Eqs. (18) and (19). The amplitude of curvature perturbations that give rise to temperature anisotropies in the CMB is constrained by Eq. (52), which imposes the condition Eq. (53). This is satisfied as long as $\alpha > 0.01$. Since we are considering values of $\alpha \simeq 1$, the contribution from the super-curvature mode will be negligible compared to that of the sub-curvature modes, regardless of Ω_0 .[‡]

Consider now the bubble wall mode contribution to the CMB anisotropies. There are two possibilities, depending on the relative strength of the gravitational effects at tunneling [15]. For $a^2b \ll 1$ we are in the weak gravity regime of Ref. [8], and the condition on the parameters becomes, from Eq. (55),

$$\gamma < 10^5 \frac{1 + 6\xi}{6\xi} \frac{M^3}{m_{\text{Pl}}^3}. \quad (59)$$

For $M \simeq 10^{-3}m_{\text{Pl}}$ this gives $\gamma < 0.03$, which is a reasonable bound on the coupling γ . On the other hand, for $a^2b \gg 1$, condition Eq. (54) is easily satisfied for $\epsilon \simeq 1/200$, see Eq. (50).

B. $\xi \gg 1$

This case was considered in Ref. [42]. The dilaton expectation value ν is much smaller than the present Planck mass. For $\xi \gg 1$, we have $\beta \simeq 4/3$ and the value of α is now determined from the required number of e -folds Eq. (28),

$$\frac{4N}{3} \simeq \alpha - \frac{4}{3} - \ln\left(\frac{1 + \alpha}{1 + 4/3}\right), \quad (60)$$

which gives $\alpha \simeq 85$. This is a regime quite different from the previous case.

We first consider the continuum spectrum of sub-curvature modes. The slow-roll parameters are

$$\epsilon \simeq 1.85 \times 10^{-4}, \quad \eta \simeq -0.016, \quad (61)$$

which determine the tilt of the primordial spectrum of density perturbations via Eq. (35) as

$$n - 1 \simeq 2\eta \simeq -0.032. \quad (62)$$

[‡]In the limit of small α and β , the e -foldings relation Eq. (28) gives $\alpha \simeq 10\sqrt{\beta}$, so the super-curvature constraint will eventually become important once $\xi \lesssim 10^{-7}$.

This is very similar to the previous case and thus compatible with large- and small-scale observations for $\Omega_0 \gtrsim 0.4$. However, the constraint on the amplitude of the angular power spectrum now determines the value of the combination λ/ξ^2 rather than λ alone, as

$$\frac{\lambda}{\xi^2} \simeq 9 \times 10^{-10}. \quad (63)$$

If we choose $\lambda \sim 1$, we have $\xi \sim 3 \times 10^4$, which gives a very reasonable expectation value for the dilaton, from Eq. (8), of

$$\nu \simeq 10^{-3} m_{\text{Pl}} \simeq 10^{16} \text{GeV}. \quad (64)$$

We now consider the de Sitter vacuum super-curvature mode. This mode also exists in this case, since $m_{\text{F}}^2 < 2H_{\text{F}}^2$ for $\alpha \gg 1$ from Eqs. (18) and (19). The amplitude of curvature perturbations is constrained by Eq. (52), which imposes the condition Eq. (53). Since we have $\alpha \gg 1$, the contribution from this super-curvature mode will be negligible.

Concerning the bubble wall mode contribution, again there are two possibilities. In the weak gravity regime $a^2 b \ll 1$, the condition on the parameters becomes

$$\gamma < 10^5 \frac{M^3}{m_{\text{Pl}}^3} \alpha^{5/2}. \quad (65)$$

which gives a trivial constraint of $\gamma \lesssim 7$ for $M \simeq 10^{-3} m_{\text{Pl}}$. For $a^2 b \gg 1$, the condition in Eq. (54) is easily satisfied for $\epsilon \simeq 10^{-4}$.

VII. MATTER ERA

One of the remaining issues is to make sure that after inflation the scalar field φ remains close to the minimum of its potential. Deviations from this would result in time variations of the gravitational constant, which are strongly constrained [43]. During the radiation era the scalar field will remain at the minimum due to the vanishing trace of the energy momentum tensor, as seen from Eq. (6). However, during the matter era the dilaton couples to the matter fluid and thus will be subject to a force which shifts the field from its minimum.

However, it is easy to show that this effect is tiny. The relevant equation, from Eq. (6), is

$$\ddot{\varphi} + 3H\dot{\varphi} + \frac{\dot{\varphi}^2}{\varphi} = \frac{4V(\varphi) - \varphi V'(\varphi) + \rho}{(1 + 6\xi)\varphi}. \quad (66)$$

For a given ρ , there is a static solution at

$$\varphi_{\text{st}}^2 = \nu^2 \left(1 + \frac{2\rho}{\lambda\nu^4} \right). \quad (67)$$

Since the matter-era energy density is tiny in comparison to the inflationary energy density which determines

$\lambda\nu^4$, the fractional shift in the gravitational constant at this static point is tiny, and so too is the energy density associated with the potential, which contributes only a minute fraction (perhaps 10^{-100} !) of the critical density.

We have analyzed the detailed behavior, described in Appendix B. When matter domination starts, the field rises from its minimum to oscillate about the static point, which it does on a very rapid timescale. As ρ decreases, the static point moves towards the true minimum (with the oscillation amplitude also decreasing though rather more slowly). At all times, the oscillations are of such small amplitude that general relativity holds to extremely high accuracy.

VIII. CONCLUSIONS

In this paper we have analyzed a variety of phenomenological constraints on a recently proposed model of open inflation in the context of induced gravity theories [20]. The most stringent constraints come from observations of the temperature anisotropies in the microwave background. The model predicts a matter power spectrum tilted to $n < 1$, which will be incompatible with observations if the universe turns out to have $\Omega_0 \lesssim 0.4$. Otherwise, it is possible to choose the parameters of the model so that it is in agreement with observations.

During the matter era, the large dilaton mass and the extremely small amplitude of oscillations around its vacuum expectation value ensure that the theory approaches general relativity very efficiently, passing all the post-Newtonian and oscillating gravitational coupling tests.

Final note: We commented in the introduction that no method had been formulated to compute the gravitational wave spectrum, which we therefore did not consider. As we were revising for the final version of this paper, preprints appeared [44] making significant progress in this direction. It will be interesting to apply these new results to specific open inflation models including the one discussed in this paper.

ACKNOWLEDGMENTS

J.G.B. was supported in part by PPARC and A.R.L. by the Royal Society. We thank Anne Green, Andrei Linde and Martin White for useful discussions. J.G.B. thanks Stanford University for its hospitality during part of this work, with the visit funded by NATO Collaborative Research Grant Ref. CRG.950760.

APPENDIX A: OPEN UNIVERSE MODE FUNCTIONS

The open universe mode functions are discussed in Refs. [14,28]

Sub-curvature modes

The sub-curvature modes can be written as [45,14]

$$\Pi_{ql}(r) = N_{ql} \tilde{\Pi}_{ql}(r), \quad (\text{A1})$$

with

$$N_{ql} = \sqrt{\frac{2}{\pi}} \prod_{n=1}^l (n^2 + q^2)^{-1/2}, \quad N_{q0} = \sqrt{\frac{2}{\pi}}, \quad (\text{A2})$$

where the unnormalized modes $\tilde{\Pi}_{ql}(r)$ can be generated from the first two

$$\tilde{\Pi}_{q0}(r) = \frac{\sin qr}{\sinh r}, \quad (\text{A3})$$

$$\tilde{\Pi}_{q1}(r) = \frac{\coth r \sin qr - q \cos qr}{\sinh r}, \quad (\text{A4})$$

through the recurrence relation

$$\begin{aligned} \tilde{\Pi}_{ql}(r) &= (2l-1) \coth r \tilde{\Pi}_{q,l-1}(r) \\ &\quad - [(l-1)^2 + q^2] \tilde{\Pi}_{q,l-2}(r). \end{aligned} \quad (\text{A5})$$

Super-curvature modes

The first ($l \geq 1$) multipoles are [34]

$$\bar{\Pi}_{11}(r) = \frac{1}{2} \left[\coth r - \frac{r}{\sinh^2 r} \right], \quad (\text{A6})$$

$$\bar{\Pi}_{12}(r) = \frac{1}{2} \left[1 + \frac{3(1-r \coth r)}{\sinh^2 r} \right]. \quad (\text{A7})$$

The rest can be obtained with the recurrence relation

$$\begin{aligned} \bar{\Pi}_{1l}(r) &= \frac{2l-1}{l-1} \coth r \bar{\Pi}_{1,l-1}(r) \\ &\quad - \frac{l}{l-1} \bar{\Pi}_{1,l-2}(r). \end{aligned} \quad (\text{A8})$$

Bubble wall modes

The first ($l \geq 2$) multipoles are [15]

$$\bar{\Pi}_{22}(r) = \frac{\sinh 4r - 8 \sinh 2r + 12r}{4 \sinh^3 r}, \quad (\text{A9})$$

$$\begin{aligned} \bar{\Pi}_{23}(r) &= \\ &= \frac{\sinh 5r - 15 \sinh 3r - 80 \sinh r + 120r \cosh r}{8 \sinh^4 r}. \end{aligned} \quad (\text{A10})$$

The rest can be obtained from the recurrence relation

$$\begin{aligned} \bar{\Pi}_{2l}(r) &= \frac{2l-1}{l-2} \coth r \bar{\Pi}_{2,l-1}(r) \\ &\quad - \frac{l+1}{l-2} \bar{\Pi}_{2,l-2}(r). \end{aligned} \quad (\text{A11})$$

APPENDIX B: MATTER ERA OSCILLATIONS OF THE GRAVITATIONAL COUPLING

Here we carry out a detailed analysis of the evolution of the dilaton during the radiation and matter eras. Here we shall assume that the oscillations are damped only by the Hubble expansion and not by any particle decays – if such decays were present the general relativistic limit would be even more quickly approached.

The energy-momentum tensor conservation Eq. (5) in the Jordan frame ensures $\rho a^{3(1+w)} = \text{constant}$ during the radiation ($w = 1/3$) and matter ($w = 0$) eras. In order to study the cosmological evolution during these eras, let us redefine our variables as

$$u = \frac{\varphi^2}{\nu^2} - 1, \quad z = mt, \quad (\text{B1})$$

where m is given by

$$m^2 = \frac{\lambda \nu^2}{1 + 6\xi}. \quad (\text{B2})$$

The φ equation of motion Eq. (6) and the Friedman equation become

$$u'' + 3 \frac{a'}{a} u' + u = \frac{2(\rho - 3p)}{\lambda \nu^4}, \quad (\text{B3})$$

$$\begin{aligned} \left[2 \frac{a'}{a} + \frac{u'}{1+u} \right]^2 &= \frac{1 + 6\xi}{6\xi} \times \\ &\left[\left(\frac{u'}{1+u} \right)^2 + \frac{u^2}{1+u} + \frac{8\rho}{\lambda \nu^4 (1+u)} \right], \end{aligned} \quad (\text{B4})$$

where primes denote derivatives w.r.t. z . During the radiation era, the right hand side of Eq. (B3) vanishes and $u = u' = 0$ is a stable fixed point. Very soon one can neglect the u -terms in the Friedman equation, and we find the radiation era attractor, $a'/a = 1/2z$. The scalar field equation of motion, $u'' + 3u'/2z + u = 0$, has an exact solution,

$$z^{1/4} u(z) = c_1 J_{\frac{1}{4}}(z) + c_2 Y_{\frac{1}{4}}(z), \quad (\text{B5})$$

where $\{J, Y\}$ are Bessel functions. Its amplitude decays asymptotically as $u(z) \propto z^{-3/4}$, so we expect the matter era to start with initial conditions at $u = u' = 0$.

During the matter era, $u = u' = 0$ is a spiral attractor and we can always neglect the u -terms in the Friedman equation,

$$\left(\frac{a'}{a} \right)^2 \simeq \left(\frac{1 + 6\xi}{6\xi} \right) \frac{A}{a^3} = \frac{4}{9z^2}, \quad (\text{B6})$$

where $A = 2\rho a^3 / \lambda \nu^4$ is a constant of order 10^{-120} in Planck units. The equation of motion for u becomes

$$u'' + \frac{2}{z} u' + u = \frac{A}{a^3} = \frac{K}{z^2}, \quad (\text{B7})$$

where $K = \beta/3$, see Eq. (27). There is an exact solution,

$$z u(z) = c_1 \sin z + c_2 \cos z + K f(z), \quad (\text{B8})$$

where $f(z)$ is related to the Sine and Cosine Integral functions by [46]

$$f(z) = \text{Ci}(z) \sin z - \text{Si}(z) \cos z = \int_0^\infty \frac{e^{-zt}}{1+t^2} dt. \quad (\text{B9})$$

The late time ($z \rightarrow \infty$) behavior of u is $u(z) \propto \sin z/z$, with a large frequency of oscillations

$$m = \left[\frac{\lambda}{8\pi\xi(1+6\xi)} \right]^{1/2} m_{\text{Pl}} \gg H_0, \quad (\text{B10})$$

and an amplitude $|u'| \sim |u| \sim A/a_0^3$, which later decays as $1/z$ at large z . The contribution of the scalar field to the total energy density is therefore suppressed by an extra factor A with respect to the ordinary matter energy density, see Eq. (B4). Since A is so tiny, there are no constraints on the parameters of the model from local experiments, see Ref. [25], and general relativity is a strong attractor of the equations of motion.

Note that during the matter era the background dilaton field oscillates very quickly, which might be thought could produce other particles, like at the end of inflation. However, due to the extremely small amplitude of oscillations, $|u| \sim A \sim 10^{-120}$, there is no significant particle production and the field's energy can only decay by redshifting away.

-
- [1] A. D. Linde, *Particle Physics and Inflationary Cosmology* (Harwood, Chur, Switzerland, 1990).
- [2] C. L. Bennett et al., *Astrophys. J.* **464**, L1 (1996).
- [3] *MAP* home page at <http://map.gsfc.nasa.gov/> (1996).
- [4] *COBRAS/SAMBA* home page at <http://astro.estec.esa.nl/SA-general/Projects/Cobras/cobras.html> (1996).
- [5] G. Jungman, M. Kamionkowski, A. Kosowsky and D. N. Spergel, *Phys. Rev. D* **54**, 1332 (1996).
- [6] J. R. Gott, *Nature*, **295**, 304 (1982); M. Sasaki, T. Tanaka, K. Yamamoto and J. Yokoyama, *Phys. Lett. B* **317**, 510 (1993).
- [7] M. Bucher, A. S. Goldhaber and N. Turok, *Phys. Rev. D* **52**, 3314 (1995); M. Bucher and N. Turok, *Phys. Rev. D* **52**, 5538 (1995).
- [8] A. D. Linde, *Phys. Lett. B* **351**, 99 (1995); A. D. Linde and A. Mezhlumian, *Phys. Rev. D* **52**, 6789 (1995).
- [9] W. L. Freedman et al., *Nature* **371**, 757 (1994); N. R. Tanvir, T. Shanks, H. G. Ferguson and D. R. T. Robinson, *Nature* **377**, 27 (1995).
- [10] J. García-Bellido, *Nucl. Phys. B Proc. Suppl.* **48**, 128 (1996); J. D. Cohn, Berkeley preprint, astro-ph/9606052 (1996).
- [11] D. H. Lyth and E. D. Stewart, *Phys. Lett. B* **252**, 336 (1990).
- [12] B. Ratra and P. J. Peebles, *Phys. Rev. D* **52**, 1837 (1995).
- [13] M. Sasaki, T. Tanaka and K. Yamamoto, *Phys. Rev. D* **51**, 2979 (1995).
- [14] D. H. Lyth and A. Woszczyna, *Phys. Rev. D* **52**, 3338 (1995).
- [15] J. García-Bellido, *Phys. Rev. D* **54**, 2473 (1996).
- [16] J. Garriga, *Phys. Rev. D* **54**, 4764, (1996);
- [17] K. Yamamoto, M. Sasaki and T. Tanaka, *Phys. Rev. D* **54**, 5031 (1996).
- [18] M. Sasaki and T. Tanaka, *Phys. Rev. D* **54**, R4705 (1996).
- [19] A. R. Liddle and D. H. Lyth, *Phys. Lett. B* **291**, 391 (1992).
- [20] A. M. Green and A. R. Liddle, *Phys. Rev. D* **55**, 609 (1996).
- [21] A. Zee, *Phys. Rev. Lett.* **42**, 417 (1979).
- [22] C. Brans and R. H. Dicke, *Phys. Rev.* **124**, 925 (1961).
- [23] S. Weinberg, *Gravitation and Cosmology* (Wiley, San Francisco, 1972).
- [24] J. García-Bellido and A. D. Linde, *Phys. Rev. D* **52**, 6730 (1995).
- [25] P. J. Steinhardt and C. M. Will, *Phys. Rev. D* **52**, 628 (1995).
- [26] J. R. Gott and T. S. Statler, *Phys. Lett.* **136B**, 157 (1984).
- [27] F. S. Accetta, D. J. Zoller and M. S. Turner, *Phys. Rev. D* **31**, 3046 (1985).
- [28] J. García-Bellido, A. R. Liddle, D. H. Lyth and D. Wands, Sussex preprint, astro-ph/9608106 (1996).
- [29] R. K. Sachs and A. M. Wolfe, *Astrophys. J.* **147**, 73 (1967).
- [30] V. F. Mukhanov, H. A. Feldman and R. H. Brandenberger, *Phys. Rep.* **215**, 203 (1992).
- [31] A. R. Liddle and D. H. Lyth, *Phys. Rep.* **231**, 1 (1993).
- [32] E. F. Bunn, D. Scott and M. White, *Astrophys. J.* **441**, L9 (1995).
- [33] E. F. Bunn and M. White, Berkeley preprint, astro-ph/9607060 (1996).
- [34] J. García-Bellido, A. R. Liddle, D. H. Lyth and D. Wands, *Phys. Rev. D* **52**, 6750 (1995).
- [35] T. Hamazaki, M. Sasaki, T. Tanaka and K. Yamamoto, *Phys. Rev. D* **53**, 2045 (1996).
- [36] J. D. Cohn, *Phys. Rev. D* **54**, 7215 (1996).
- [37] K. Yamamoto and E. F. Bunn, *Astrophys. J.* **461**, 8 (1996).
- [38] K. Górski, B. Ratra, R. Stompor, N. Sugiyama and A. J. Banday, Max Planck preprint, astro-ph/9608054 (1996).
- [39] A. R. Liddle, D. H. Lyth, D. Roberts and P. T. P. Viana, *Mon. Not. Roy. Astr. Soc.* **278**, 644 (1996).
- [40] M. White and J. Silk, *Phys. Rev. Lett.* **77**, 4704 (1996).
- [41] A. Dekel, *Ann. Rev. Astron. Astrophys.* **32**, 371 (1994).
- [42] B. Spokoiny, *Phys. Lett.* **129B**, 39 (1984).
- [43] C. M. Will, *Theory and Experiment in Gravitational Physics*, Cambridge University Press (Cambridge, 1993).
- [44] T. Tanaka and M. Sasaki, Osaka preprint, astro-ph/9701053 (1997); M. Bucher and J. D. Cohn, Stony Brook preprint, astro-ph/9701117 (1997).
- [45] E. R. Harrison, *Rev. Mod. Phys.* **39**, 862 (1967); M. L.

- Wilson, *Astrophys. J.* **273**, 2 (1983); L. F. Abbott and R. K. Schaefer, *Astrophys. J.* **308**, 546 (1986).
- [46] M. Abramowitz and I. Stegun, *Handbook of Mathematical Functions*, (Dover, 1965), p.232.